Catalytic Oxidation

DOI: 10.1002/anie.201202034

Alkali-Metal-Promoted Pt/TiO_2 Opens a More Efficient Pathway to Formaldehyde Oxidation at Ambient Temperatures**

Changbin Zhang, Fudong Liu, Yanping Zhai, Hiroko Ariga, Nan Yi, Yongchun Liu, Kiyotaka Asakura, Maria Flytzani-Stephanopoulos, and Hong He**

Formaldehyde is emitted from building and furnishing materials and consumer products,[1] and is known to cause irritation of eyes and respiratory tract, headache, pneumonia, and even cancer.[2,3] It is a dominant indoor air pollutant, especially in developing countries, and significant efforts have gone into indoor HCHO purification to meet environmental regulations and human health needs.

Removal of HCHO by adsorbents has been investigated extensively using potassium permanganate, activated carbon, aluminum oxide, and some ceramic materials.[4–6] Sorbent effectiveness is typically limited by low adsorption capacities. Catalytic oxidation is the most effective technology for volatile organic compound (VOC) abatement because VOCs can be oxidized to CO_2 over certain catalysts at much lower temperatures than in thermal oxidation.[7–9] Supported noble metal catalysts (Pt, Pd, Rh, Au, Ag) or metal oxide catalysts (Ni, Cu, Cr, Mn) have been used for the catalytic oxidation of VOCs.[8–22] Complete oxidation of HCHO over catalysts occurs above 150 °C on clean and oxidized films of Ni, Pd, and Al[15] and over silver–cerium composite oxide,[16] above 100 °C over $Ag/MnOx\text{-}CeO_2$[18] and Au/CeO_2,[19] and above 85 °C over $Pd\text{-}Mn/Al_2O_3$[17] and Au/FeOx.[20]

As catalytic oxidation at even lower temperatures is desirable for indoor air purification, the development of a catalyst for total HCHO oxidation at room temperature is of great interest. In our recent study,[21,22] 1% Pt/TiO_2 catalyst was shown to be effective for HCHO oxidation at room temperature, achieving 100% conversion of $\delta = 100$ ppm HCHO to CO_2 and H_2O at a gas hourly space velocity (GHSV) of 50000 h^{-1}. However, we also observed that this type catalyst is not as active as needed for practical applications, and deactivates with time-on-stream.

Herein, we report a novel alkali-metal-promoted Pt/TiO_2 catalyst for the ambient destruction of HCHO. We show that the addition of alkali-metal ions (such as Li^+, Na^+, and K^+) to Pt/TiO_2 catalyst stabilized an atomically dispersed Pt-O(OH)x–alkali-metal species on the catalyst surface and also opened a new low-temperature reaction pathway, significantly promoting the activity for the HCHO oxidation by activating H_2O and catalyzing the facile reaction between surface OH and formate species to total oxidation products.

Figure 1a shows the HCHO conversion to CO_2 as a function of temperature over the x% Na-1% Pt/TiO_2 ($x = 0$, 1, and 2) samples at a GHSV of 120000 h^{-1} and HCHO inlet of $\delta = 600$ ppm. All gas streams were humidified to a RH of around 50%. Before each activity test, the samples were reduced in H_2 at 300 °C for 30 min. The sodium-free catalyst had low activity for the HCHO oxidation reaction, with HCHO conversion being only about 19% at 15 °C. With 1% Na addition, the HCHO conversion reached 96% at 15 °C and 100% at 40 °C. With 2% Na addition, 100% HCHO conversion to CO_2 and H_2O was measured at 15 °C. The effect of Na addition on the surface reducibility was examined by H_2 temperature-programmed reduction (TPR; Figure 1b). The amounts of H_2 consumption were about the same over all the samples, but the addition of Na shifted the reduction peak to lower temperatures, that is, from 2 °C for 1% Pt/TiO_2 to −6 °C for 1% Na-1% Pt/TiO_2 and −11 °C for 2% Na-1% Pt/TiO_2. Thus, the sample reducibility correlates with the sample activity. The most active 2% Na-promoted sample had excellent stability as checked by long isothermal tests. For example, at a GHSV of 300000 h^{-1} and with the same other reaction conditions, approximately 80% HCHO conversion was maintained over a 72 h-long test (Figure 1a, inset). Li and K were equally effective promoters to Na and imparted the same high activity and stability to the Pt species (Supporting Information, Figure S1). Water vapor and oxygen effects on the activity of $Na\text{-}Pt/TiO_2$ are important (Supporting Information, Figures S2, S3).

Deionized-water washing of the samples was performed to check the alkali-metal and Pt interaction. While most of the Na was removed from the Na- containing catalysts, a residual amount remained (Supporting Information, Table S1). Activity test results (Supporting Information, Figure S1) showed that the washed catalyst had identical activity for HCHO

[*] C. Zhang, F. Liu, Y. Liu, Prof. H. He
Research Center for Eco-Environmental Sciences
Chinese Academy of Sciences
Shuangqing Road 18, Beijing, 100085 (China)
E-mail: honghe@rcees.ac.cn
Y. Zhai, N. Yi, Prof. M. Flytzani-Stephanopoulos
Department of Chemical and Biological Engineering
Tufts University, Medford, MA 02155 (USA)
E-mail: mflytzan@tufts.edu
H. Ariga, Prof. K. Asakura
Catalysis Research Center, Hokkaido University (Japan)

[**] The authors appreciate the valuable advices of Emeritus Prof. Kenichi Tanaka of Tokyo University and the aberration-corrected HAADF/STEM tests performed by Dr. David Bell of the School of Engineering and Applied Sciences, Harvard University. This work was supported by the National Natural Science Foundation of China (50921064 and 21077117), the Program of the Ministry of Science and Technology of China (2010AA064905), the Photon Factory, KEK (Japan) (2009G177), and the BL14W1 beam line, Shanghai Synchrotron Radiation Facility. Work at Tufts University was supported by the U.S. Department of Energy (DOE)/Basic Energy Sciences (BES) Grant No. DE-FG02-05ER15730.

Supporting information for this article is available on the WWW under http://dx.doi.org/10.1002/anie.201202034.

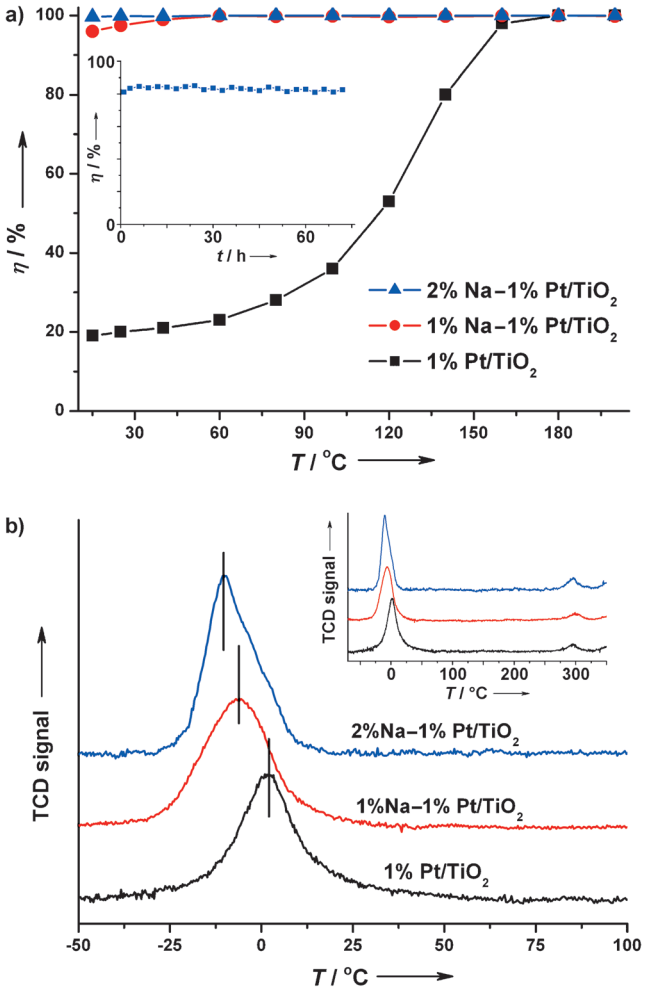

Figure 1. a) HCHO conversion η over x wt% Na-1 wt% Pt/TiO_2 ($x=0$, 1, and 2) catalysts as a function of temperature T. Reaction conditions: HCHO $\delta=600$ ppm, O_2 20 vol%, relative humidity: about 50%, He balance, total flow rate of 50 $cm^3\,min^{-1}$, and GHSV 120000 h^{-1} (inset: stability test of 2% Na-1% Pt/TiO_2 at 25 °C, GHSV 300000 h^{-1} with same other reaction conditions). b) H_2 TPR profiles of x wt% Na-1% Pt/TiO_2 ($x=0$, 1, and 2).

oxidation to the unwashed sample. Thus, only a small amount of Na is needed to promote the Pt on the surface (9.6 at.% Na for 1.2 at.% Pt; Supporting Information, Table S1). In turn, the Pt binds the residual Na and stabilizes it. Indeed, it is the Pt, not the TiO_2 surface, that binds the Na, because in the absence of Pt all Na is removed by washing (see the Supporting Information for the washing procedure). The residual amount of Na on the sample surface, measured by XPS (Supporting Information, Table S1), was significantly higher for the most active catalyst sample corresponding to a Na/Pt atomic surface ratio of 8:1. These findings are similar to what has been reported for Pt/SiO_2, when promoted by alkali-metal oxides.[23] In that work it was shown that the Na-O-Pt interaction is present only for the sub-nm size Pt species. Pt-$O(OH)_x$-Na clusters were proposed as the active sites for the water-gas shift reaction.[23] The promoted catalyst differs from the unpromoted catalyst in that it has alkali-metal-stabilized hydroxyl species in close proximity to the Pt site.[23,24]

Huang et al.[25,26] also studied the catalytic oxidation of HCHO over Pt/TiO_2 and Pd/TiO_2 catalysts at ambient temperatures. They observed that the $NaBH_4$-reduced Pd/TiO_2 samples showed higher catalytic activity than H_2-reduced ones; but did not discuss the activity enhancement as an alkali-metal promotion. It would be worth exploring whether a sodium promotion effect as the one described here for Pt is also manifested for Pd catalysts.

Detailed catalyst sample characterization was conducted and is shown in the Supporting Information, Figure S5–S14. XAFS measurements were conducted to study the structure of samples before/after Na addition and before/after H_2 reduction under atmospheric pressure. The XANES and EXAFS of Ti-K and Pt-L_{III} edges were recorded in transmission mode at room temperature. Both XANES and EXAFS results of the Ti-K edge in x% Na-Pt/TiO_2 catalysts (Supporting Information, Figure S7–S9) showed no change before and after Na addition or H_2 reduction. In contrast, clear distinctions were observed for the Pt-L_{III} edge with and without Na addition. From the Pt-L_{III} XANES spectra and their first-order derivatives (Supporting Information, Figure S10–S12), we can see that before H_2 reduction, the Pt species in all samples were in oxidized state by comparing the white line intensity with those of Pt foil and PtO_2. The Pt species were reduced to metallic state after in situ reduction. With further exposure to ambient air, the Pt species became partially oxidized. In particular, the Pt species in the Na-doped samples were more oxidized than those in Pt/TiO_2, which is probably due to the formation of Pt-$(ONa)_x$ species with strong association.[23,24]

The curve fitted k^3-weighted EXAFS oscillations of the Pt L_{III} edges along with the corresponding transformations into R space and as measured k^3-weighted EXAFS oscillations are presented in the Supporting Information, Figures S13 and S14, and the fitting parameters are given in Table 1. Prior to H_2 reduction, all of the Pt was coordinated with O or Cl, and the Pt-Pt coordination was zero on all catalysts. After in situ H_2 reduction at 300 °C, all of the Pt species were reduced to the metallic phase, yet the Pt-Pt coordination number was monotonically lowered with an increase in the amount of Na. The relationship between Pt particle size and Pt-Pt coordination number determined by EXAFS is well-established,[27] whereby the metal–metal coordination number is a function of the total number of metal atoms in one particle and a smaller coordination number corresponds to a smaller particle size.[28] Thus, the EXAFS findings show that Na addition effectively reduces the particle size of Pt from 10 Å (Na-free), to 6.8 Å (1% Na), to 4.8 Å nm (2% Na). With higher (2%) amount of Na as in the most active catalyst sample, the decrease of Pt cluster size was also confirmed by the STEM images and corresponding particle size distributions (Supporting Information, Figure S6). Single Pt atoms or ions are also stabilized on these surfaces. Once the prereduced catalysts were exposed to air, as in realistic operation for HCHO oxidation, surface structures were changed owing to oxygen adsorption[29] and the structural differences were substantial among three samples. The Na-free Pt/TiO_2 sample

Table 1: Fitting parameters of the curve fitted k^3-weighted EXAFS analysis of x% Na-1% Pt/TiO_2 (x=0, 1, 2).[a]

Samples	Shell	CN	R [Å] (±0.01)	DW [Å]	R factor
Pt-foil	Pt-Pt	12.0±2.3	2.77	0.077±0.010	0.8
PtO_2	Pt-O	6.0±1.2	2.02	0.061±0.020	3.0
	Pt-O-Pt	4.0±1.0	3.14	0.061±0.012	
1Pt/TiO_2[b]	Pt-O	3.7±1.2	2.02	0.061±0.020	0.6
	Pt-Cl	2.3±1.0	2.30	0.051±0.057	
1Na-1Pt[b]	Pt-O	6.0±1.3	2.02	0.061±0.020	4.1
2Na-1Pt[b]	Pt-O	5.4±1.2	2.02	0.061±0.020	8.7
1Pt/TiO_2[c]	Pt-Pt	5.6±1.2	2.77	0.097±0.010	1.3
1Na-1Pt[c]	Pt-Pt	3.8±0.8	2.77	0.097±0.010	2.3
2Na-1Pt[c]	Pt-Pt	2.4±0.5	2.77	0.097±0.010	7.2
1Pt/TiO_2[d]	Pt-Pt	4.7±1.0	2.77	0.097±0.010	0.4
	Pt-Cl	0.6±0.2	2.30	0.051±0.057	
1Na-1Pt[d]	Pt-Pt	2.7±0.6	2.77	0.097±0.010	11.6
	Pt-O	1.3±0.3	2.02	0.061±0.020	
2Na-1Pt[d]	Pt-O	2.8±0.6	2.02	0.092±0.010	9.8

[a] CN = coordination number, R = bond length, DW = Debye–Waller factor, Pt-Pt is the coordination shell in Pt metal, Pt-O is the first coordination shell in PtO_2, Pt-O-Pt is the second coordination shell in PtO_2. [b] Samples calcined in static air, 400 °C, 2 h. [c] Samples after in situ H_2 reduction in 10% H_2/Ar at 300 °C for 30 min. [d] Samples exposed to ambient air after H_2 reduction.

showed a Pt-Pt coordination shell in Pt metal and a small residual Pt-Cl coordination shell (the absence of residual Cl effect on the activity of Na-Pt/TiO_2 is shown and discussed in the Supporting Information, Table S3, Figure S4). Addition of Na into the catalyst clearly decreased the Pt-Pt and eliminated the Pt-Cl shell fraction, while it increased the Pt-O shell fraction. With 2% Na added, only a Pt-O shell was detected, hence 2% Na addition can completely suppress the formation of Pt-Pt bonds in the presence of O_2 and stabilizes atomically dispersed Pt-O species on the TiO_2 surface. Furthermore, the Pt-O coordination number in this sample was only about 3; that is, much lower than the normal coordination number in PtO_2. A Bader charge closer to PtO was calculated by DFT[23] for the single Pt cation-centered $K_6PtO_4(OH)_2$ cluster that was proposed as the active site for the low-temperature water-gas shift reaction. A similar structure may be responsible for the ambient HCHO oxidation reaction.

Qiao et al. recently reported a novel catalyst that consisted of atomically dispersed Pt atoms on FeO_x support for CO oxidation.[30] As the catalyst was prepared with a co-precipitation method using sodium carbonate as precipitant and $H_2PtCl_6{\cdot}6H_2O$ as Pt precursor, the presence of Na species possibly also played an important role in the fabrication of this single-atom Pt catalyst.

The reaction mechanism of HCHO oxidation on Na-free Pt/TiO_2 catalysts has been investigated at room temperature.[22] As shown in Figure 2a, formate species (1570, 1359 cm^{-1} for $\upsilon(COO^-)$ and 2956, 2868, 2740 cm^{-1} for $\upsilon(CH)$)[22,31] were formed and were dominant on Pt/TiO_2 after the catalyst was exposed to a flow of O_2 + HCHO + He + H_2O for 60 min. With helium purging for 60 min, the formate species completely decomposed into CO species (2058, 1769 cm^{-1}).[22] Upon catalyst exposure to O_2, the CO species were converted into CO_2 and desorbed from the

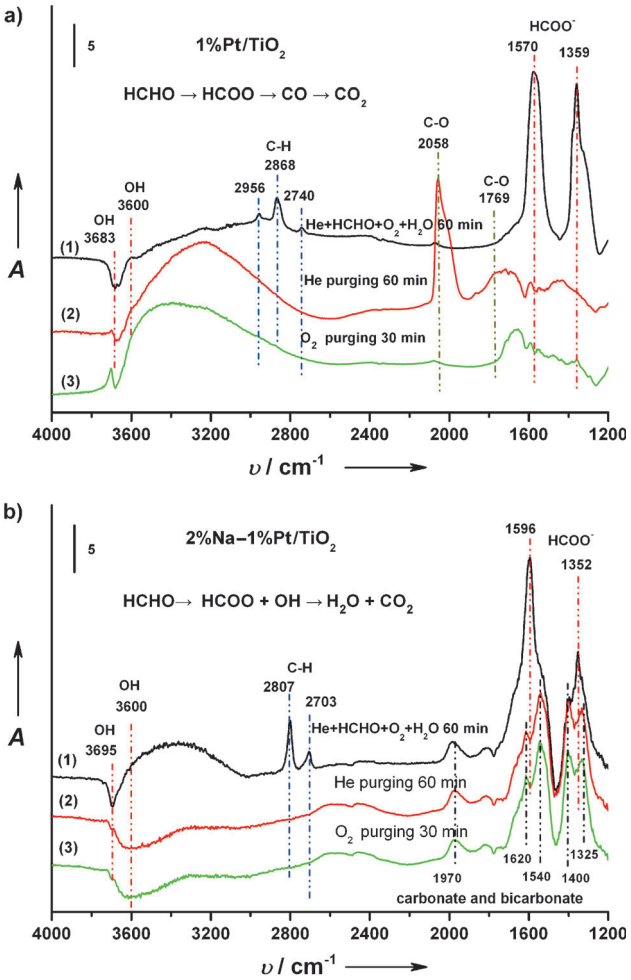

Figure 2. In situ DRIFTS over a) 1% Pt/TiO_2 and b) 2% Na-1% Pt/TiO_2 after 1) a flow of He + HCHO + O_2 + H_2O for 60 min followed by 2) He purging for 60 min, and finally 3) O_2 purging for 30 min at room temperature. For the dynamic time sequence of the DRIFTS spectra, see the Supporting Information, Figure S15. Reaction conditions: HCHO δ = 600 ppm, O_2 20 vol%, about 50% relative humidity, He balance, total flow rate of 50 $cm^3\,min^{-1}$.

surface. Therefore, it was concluded that the HCHO oxidation reaction on sodium-free samples follows the formate ($HCOO^-$) decomposition route (HCHO → $HCOO^-$ → CO → CO_2), with formate decomposing into CO being the rate-determining step.[22] Kim et al. also reported a similar reaction mechanism of HCHO oxidation over Pt/TiO_2 catalyst at room temperature.[32]

Here, the reaction mechanism of HCHO oxidation over Na-promoted Pt/TiO_2 catalysts was studied using in situ DRIFTS (Figure 2b; Supporting Information, Figure S15). After the samples were exposed to a flow of O_2 + HCHO + He + H_2O for 60 min, surface formate (1596, 1352 cm^{-1} for $\upsilon(COO^-)$ and 2807, 2703 cm^{-1} for $\upsilon(CH)$,[33] were dominant at steady-state. Two kinds of surface hydroxyl (OH) groups at ca. 3695 and 3600 cm^{-1} were observed on the catalyst surface. The negative peak of OH species at 3695 cm^{-1} suggests that the formation of surface $HCOO^-$ consumed some OH species (Supporting Information, Figure S15A). With He purging (Supporting Information, Figure S15B), the intensities of the

$HCOO^-$ and OH peaks at 3600 cm^{-1} dropped simultaneously. After 60 min, the $HCOO^-$ species completely disappeared from the surface and the OH peak at 3600 cm^{-1} became negative (Figure 2b), indicating the complete reaction between formate and active OH groups. In contrast, surface carbonate and bicarbonate species (1970, 1620, 1540, 1400, and 1325 cm^{-1})[34] remained unchanged and gradually increased with formate consumption (Figure 2b). A further O_2 purge did not alter the spectra, showing that no further reaction occurred. Based on these results, we conclude that HCHO oxidation over the promoted 2% Na-1% Pt/TiO_2 catalyst follows a new pathway, that is, the direct formate oxidation ($HCHO \rightarrow HCOO + OH \rightarrow H_2O + CO_2$), and the reaction between surface hydroxyls and formate is preferred over the decomposition of formate to CO followed by CO oxidation.

To further check for the new HCHO oxidation pathway, we carried out kinetics tests with both the sodium-free and sodium-promoted Pt/TiO_2 catalysts. Figure 3 shows Arrhenius-type plots for the rates of HCHO oxidation over the 1% Pt/TiO_2 and 2% Na-1% Pt/TiO_2 (unwashed and washed) samples. The apparent activation energy of the reaction on the sodium-free sample is (30 ± 4) kJ mol^{-1}; however, over the Na-Pt/TiO_2 catalyst, in both the unwashed and washed state, the reaction was easier to activate, with apparent activation energy of about (13 ± 4) kJ mol^{-1}, thus providing further evidence that the reaction pathway was changed on the sodium-promoted samples.

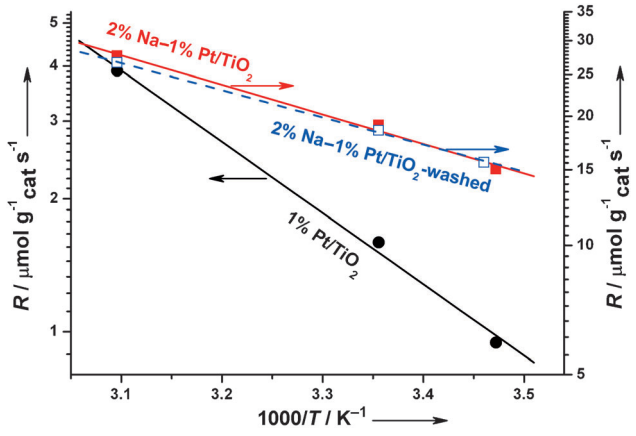

Figure 3. HCHO oxidation rate *R* over 1% Pt/TiO_2, 2% Na-1% Pt/TiO_2 and 2% Na-1% Pt/TiO_2-washed catalysts.

HCHO temperature-programmed desorption (HCHO-TPD) tests were conducted to further probe how the mechanism of HCHO oxidation is altered by Na addition onto Pt/TiO_2. Figure 4 presents the HCHO-TPD profiles collected from the 1% Pt/TiO_2 and 2% Na-1% Pt/TiO_2 samples as a function of temperature (0–120 °C). Over the sodium-free sample (Figure 4a), CO was the only carbon-containing product and no CO_2 was detected, showing that over the sodium-free sample the HCHO dehydrogenation route ($HCHO \rightarrow H_2 + CO$) is followed. By contrast, CO_2 is the major product over the sodium-modified sample even at

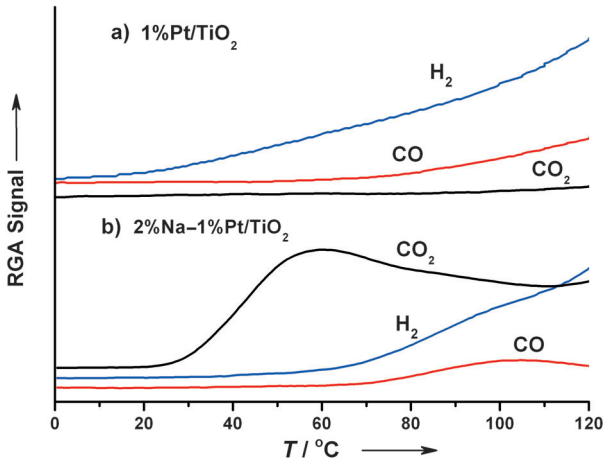

Figure 4. Profiles of species detected by temperature-programmed desorption of HCHO from a) 1% Pt/TiO_2 and b) 2% Na-1% Pt/TiO_2 samples as a function of temperature (0–120 °C). For detailed experimental information, see the Supporting Information.

room temperature (Figure 4b), indicating that Na addition changes the reaction pathway. Additionally, we observed that a small amount of CO and H_2 was produced at higher temperatures (> 70 °C) over the sodium-doped catalyst. This can be explained by the dehydrogenation pathway becoming more dominant (easier) at high temperatures. Thus, we again conclude that the preferred ambient temperature pathway for HCHO oxidation is through formate oxidation by the abundant associated hydroxyl groups on the Pt-$O(OH)_x$Na-type clusters.

Cyclic CO-TPR was performed to check whether on the sodium-promoted Pt/TiO_2 catalyst the activation of the surface OH species is enhanced (Supporting Information, Figure S16). Only a small amount of active OH groups existed on the 1% Pt/TiO_2 surface to react with CO to produce CO_2 and H_2 ($2CO + 2OH \rightarrow 2CO_2 + H_2$) at about 150 °C. By contrast, a considerable number of active OH groups were present on the sodium-promoted sample, which could react with CO at about 100 °C, indicating that Na addition increased the concentration of surface OH groups. With intermittent rehydration at ambient conditions, the second CO-TPR cycle was identical to the first. Thus, the OH groups were fully regenerated on the catalyst surface. These findings are the same as what has been reported for sodium-promoted Pt/SiO_2 for the low-temperature water-gas shift reaction.[23] The promotion is structural in the WGS reaction; that is, the CO + OH reaction is similarly activated on all Pt catalysts and is independent of the type of support. A similar apparent activation for promoted and unpromoted Pt catalysts was reported.[23] However, the case of HCHO oxidation on the same type catalyst is distinct in that the addition of alkali metal alters the pathway from the HCHO decomposition followed by CO oxidation to that of direct formate oxidation. When a catalyst lacks OH groups, the formate species tend to decompose into surface CO (HCOO-M → CO-M + OH-M).[22] However, when a large amount of nearby OH groups is present, the formate decomposition is inhibited and the direct formate oxidation (HCOO-M + OH-M → H_2O +

$CO_2 + 2\,M$) is facilitated. We found that the OH groups are regenerated by the H_2O vapor on stream. Therefore, we conclude that the regenerable OH provided by Na addition on the Na-Pt/TiO_2 sample, are responsible for altering the HCHO oxidation reaction pathway.

On the basis of the above results, we propose that the key steps for HCHO oxidation over the alkali-metal-promoted Pt/TiO_2 catalyst (including O_2, HCHO, and H_2O activation) take place on the atomically dispersed Pt-$O(OH)_x$ alkali-metal species, which alters the ambient-temperature HCHO oxidation pathway by promoting the reaction between surface OH and formate species at room temperature, and thus greatly enhancing the HCHO oxidation activity. Such OH activation by alkali-metal ion addition may apply to other volatile organic compound oxidation reactions and to other metals.

Experimental Section

The x wt% Na-1 wt% Pt/TiO_2 ($x = 0$, 1, and 2) catalysts were prepared at room temperature by excess solution impregnation of an anatase TiO_2 powder (Millennium Inorganic Chemicals, BET surface area of 69 m^2g^{-1}), using an aqueous solution of $PtCl_4$ (Sigma–Aldrich) and Na/K carbonate or $LiNO_3$ solution (Sigma–Aldrich). After impregnation, excess water was removed in a rotary evaporator at 30–60 °C under vacuum until dryness. Samples were dried at 110 °C for 12 h and calcined at 400 °C in static air for 2 h (5 °C min^{-1}). After calcination, the samples were subjected to 10% H_2/Ar (50 mL min^{-1}) reduction at 300 °C for 30 min before testing.

The activity tests and kinetics measurements for the catalytic oxidation of HCHO over the catalysts were performed in a fixed-bed quartz flow reactor. The feed gas composition for the activity tests was HCHO/O_2/He = 600 ppm/20 vol%/balance and 50% relative humidity (total flow 50 mL min^{-1}) at a gas hourly space velocity of 120000/300000 h^{-1} ($W/F = 0.018/0.0072$ g s cm^{-3}). For kinetics measurement, the feed gas composition was HCHO/O_2/He = 700 ppm/20 vol%/balance and 50% relative humidity (total flow 175 mL min^{-1}) for the reactor operated in a differential mode, keeping the HCHO conversion below 15%. The inlet and outlet gases were monitored by FTIR (Nicolet 380) equipped with IR-cells with 2 m of light pass.

Received: March 14, 2012
Revised: June 10, 2012
Published online: August 29, 2012

Keywords: alkali metals · catalytic oxidation · formaldehyde · platinum · titanium dioxide

[1] C. Yu, D. Crump, *Build. Environ.* **1998**, *33*, 357 – 374.
[2] J. J. Collins, R. Ness, R. W. Tyl, N. Krivanek, N. A. Esmen, T. A. Hall, *Regul. Toxicol. Pharm.* **2001**, *34*, 17 – 34.
[3] A. P. Jones, *Atmos. Environ.* **1999**, *33*, 4535 – 4564.
[4] B. Eriksson, L. Johanssin, I. Svedung, *The Nordest Symposium on Air Pollution Abatement by Filtration and Respiratory Protection*, Copenhagen, **1980**.
[5] D. Arthur, Little Inc., "*A Report to the HCHO Institute by Arthur D. Little Inc.*", Cambridge, MA, **1981**.
[6] Y. Sekine, A. Nishimura, *Atmos. Environ.* **2001**, *35*, 2001 – 2007.
[7] J. J. Spivey, *Ind. Eng. Chem. Res.* **1987**, *26*, 2165 – 2180.
[8] S. Scirè, S. Minicò, C. Crisafulli, S. Galvagno, *Catal. Commun.* **2001**, *2*, 229 – 232.
[9] S. Scirè, S. Minicò, C. Crisafulli, C. Satriano, A. Pistone, *Appl. Catal. B* **2003**, *40*, 43 – 49.
[10] J. E. Sawyer, M. A. Abraham, *Ind. Eng. Chem. Res.* **1994**, *33*, 2084 – 2089.
[11] P. Papaefthimiou, T. Ioannides, X. E. Verykios, *Catal. Today* **1999**, *54*, 81 – 92.
[12] W. Wang, H. B. Zhang, G. D. Lin, Z. T. Xiong, *Appl. Catal. B* **2000**, *24*, 219 – 232.
[13] E. M. Cordi, J. L. Falconer, *Appl. Catal. A* **1997**, *151*, 179 – 191.
[14] C. Reed, Y. K. Lee, S. T. Oyama, *J. Phys. Chem. B* **2006**, *110*, 4207 – 4216.
[15] J. M. Saleh, S. M. Hussian, *J. Chem. Soc. Faraday Trans.* **1986**, *82*, 2221 – 2234.
[16] S. Imamura, D. Uchihori, K. Utani, *Catal. Lett.* **1994**, *24*, 377 – 384.
[17] M. C. Álvarez-Galván, V. A. de La Peña O'Shen, J. L. G. Fierro, P. L. Arias, *Catal. Commun.* **2003**, *4*, 223 – 228.
[18] X. Tang, J. Chen, Y. Li, Y. Li, Y. Xu, W. Shen, *Chem. Engin. J.* **2006**, *118*, 119 – 125.
[19] M. Jia, H. Bai, Zhaorigetu, Y. Shen, Y. Li, *J. Rare Earths* **2008**, *26*, 528 – 531.
[20] C. Li, Y. Shen, M. Jia, S. Sheng, M. O. Adebajo, H. Zhu, *Catal. Commun.* **2008**, *9*, 355 – 361.
[21] C. Zhang, H. He, K. Tanaka, *Catal. Commun.* **2005**, *6*, 211 – 214.
[22] C. Zhang, H. He, K. Tanaka, *Appl. Catal. B* **2006**, *65*, 37 – 43.
[23] Y. Zhai, D. Pierre, R. Si, W. Deng, P. Ferrin, A. U. Nilekar, G. Peng, J. A. Herron, D. C. Bell, H. Saltsburg, M. Mavrikakis, M. Flytzani-Stephanopoulis, *Science* **2010**, *329*, 1633 – 1636.
[24] X. Zhu, M. Shen, L. L. Lobban, R. G. Mallinson, *J. Catal.* **2011**, *278*, 123 – 132.
[25] H. Huang, D. Y. C. Leung, *J. Catal.* **2011**, *280*, 60 – 67.
[26] H. Huang, D. Y. C. Leung, *ACS Catal.* **2011**, *1*, 348–354.
[27] B. J. Kip, F. B. M. Duivenvoorden, D. C. Koningsberger, R. Prins, *J. Catal.* **1987**, *105*, 26 – 38.
[28] R. B. Greegor, F. W. Lytle, *J. Catal.* **1980**, *63*, 476 – 486.
[29] F. Tao, S. Dag, L. Wang, Z. Liu, D. R. Butcher, H. Bluhm, M. Salmeron, G. A. Somorjai, *Science* **2010**, *327*, 850 – 853.
[30] B. Qiao, A. Wang, X. Yang, L. F. Allard, Z. Jiang, Y. Cui, J. Liu, J. Li, T. Zhang, *Nat. Chem.* **2011**, *3*, 634 – 641.
[31] J. Raskó, T. Kecskés, J. Kiss, *J. Catal.* **2004**, *224*, 261 – 268.
[32] S. S. Kim, K. H. Park, S. C. Hong, *Appl. Catal. A* **2011**, *398*, 96 – 103.
[33] http://webbook.nist.gov/cgi/cbook.cgi?Formula = HCOONa&NoIon = on&Units = SI&cIR = on#IR-Spec.
[34] http://webbook.nist.gov/cgi/cbook.cgi?ID = B6007910&Units = SI&Mask = 80.

